UCRL JC 134224
UCRL-JC-
PREPRINT

Role of λ-Diagrams in Estimating Porosity and Saturation from Seismic Velocities

James G. Berryman
Patricia A. Berge
Brian P. Bonner

This paper was prepared for submittal to
Geophysics

May, 1999

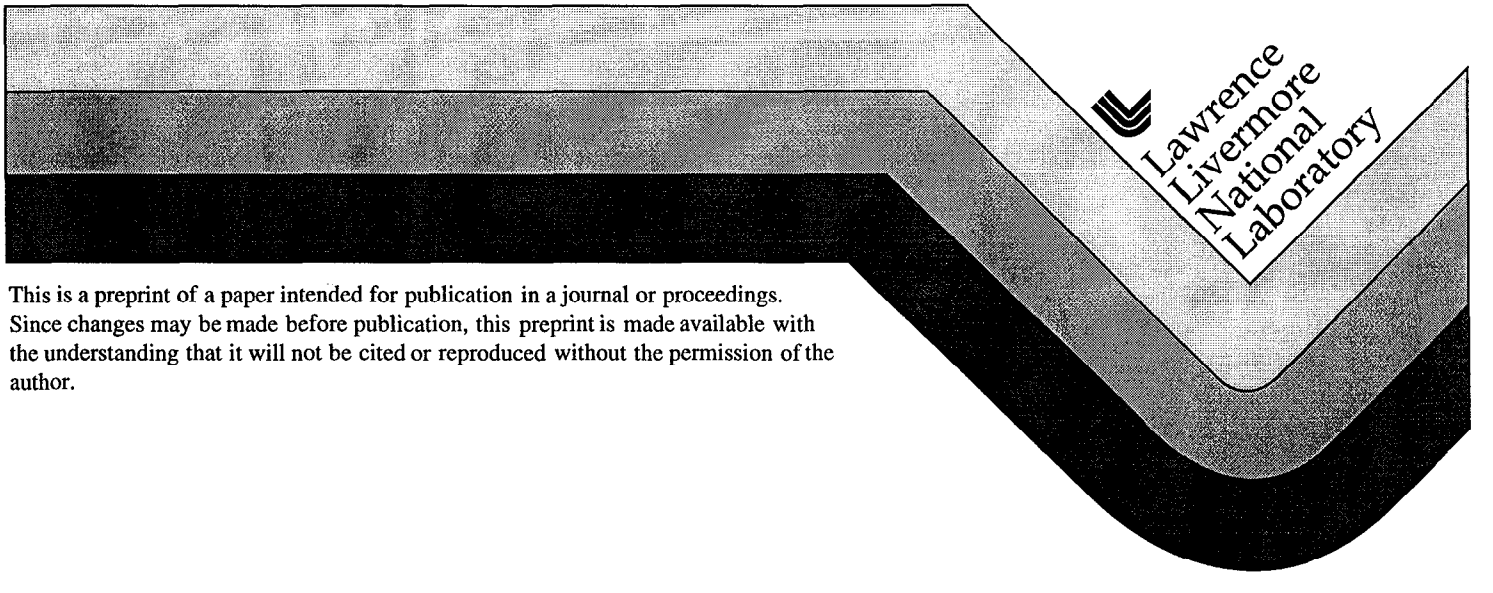

Role of λ-Diagrams in Estimating Porosity and Saturation from Seismic Velocities

James G. Berryman, Patricia A. Berge, and Brian P. Bonner, Lawrence Livermore National Laboratory

Summary

Two of the most difficult to measure properties of subsurface rocks and fluids are porosity and saturation level. We present a new method of estimating both porosity and saturation level from seismic data, by displaying data on plots emphasizing the Lamé parameter λ, determined from measured P and S velocities. A mathematical trick associated with one plotting method produces universal and easily interpretable behavior for sedimentary and igneous rocks, various unconsolidated materials, and man-made materials, in that virtually all the seismic data analyzed plot along straight lines. The slopes of these lines correlate well with porosity, while the locations of the data points along the lines provide estimates of fluid saturation.

Introduction

When liquid or gas completely fills interconnnecting voids, a well-known result due to Gassmann (1951) predicts how the composite elastic constants that determine P and S velocities should depend on the fluid and drained rock or soil elastic constants and densities. Gassmann's is a low frequency result and both well-log and laboratory measurements of wave velocities at sonic and ultrasonic frequencies have been observed to deviate markedly from Gassmann's predictions. This is especially so for partial saturation conditions. In some cases these deviations can be attributed to "patchy saturation," meaning that some void regions are fully saturated with liquid and others are filled only with gas, so that Gassmann's formulas apply locally (but not globally) and must be averaged to obtain the overall seismic velocity of the system. In other cases, neither Gassmann's formulas nor the "patchy saturation" model seem to apply to measured velocity data.

Simple algebraic expressions relate the seismic P and S velocities v_p and v_s to the Lamé parameters λ and μ of elasticity theory, and the overall density ρ. These relationships are well-known, but the parameter λ is seldom used to analyze seismic data. Our first new way of displaying seismic data is to plot data points in the $(\rho/\mu, \lambda/\mu)$-plane. The advantage of this plot is that, when either homogeneous mixing of fluids or full segregation of fluids (*i.e.*, Gassmann behavior or the simplest form of patchy saturation) applies, most of the data will fall on one of two straight lines. Significant deviations from these two expected behaviors then provide a clear indication that the data violate some of the assumptions in Gassmann's simple model. Our second innovation in displaying seismic data is to plot the points in the $(\rho/\lambda, \mu/\lambda)$-plane. This second approach involves the use of an easily understood mathematical trick that leads naturally to universal and easily interpreted behavior; virtually all laboratory data on partial saturation we have analyzed plot with minimal scatter along straight lines in this plane. The length and slope of these lines have quantitative implications for measurements of both partial saturation and porosity.

Basics of elastic wave propagation

For isotropic elastic materials, the two bulk elastic wave speeds are compressional $v_p = \sqrt{(\lambda + 2\mu)/\rho}$ and shear $v_s = \sqrt{\mu/\rho}$. Here the Lamé parameters λ and μ are the constants that appear in Hooke's law relating stress to strain in an isotropic material. For a porous system with porosity ϕ, the overall density of the rock or sediment is just the volume weighted density given by $\rho = (1-\phi)\rho_s + \phi[S\rho_l + (1-S)\rho_g]$, where ρ_s, ρ_l, ρ_g are the densities of the constituent solid, liquid and gas, respectively, and S is the liquid saturation (Domenico, 1976). When liquid and gas are distributed uniformly in all pores and cracks, Gassmann's equations say that, for quasistatic isotropic elasticity and low frequency wave propagation, the shear modulus μ will be mechanically independent of the properties of any fluids present in the pores, while the overall bulk modulus $\lambda + \frac{2}{3}\mu$ of the rock or sediment including the fluid depends in a known way on porosity and elastic properties of the fluid and dry rock or sediment. Thus, in the Gassmann model, the Lamé parameter λ is elastically *dependent* on fluid properties, while μ is not. The effect of the liquid on λ is negligible until full saturation is approached. Both v_p and v_s will decrease with increasing fluid saturation due to the increasing density. While nearing full saturation, the shear velocity continues its downward trend, but the compressional velocity suddenly shoots up to its full saturation value. An example (Murphy, 1984) of one such plot of velocity vs. saturation is shown in Fig. 1a. This is the expected (ideal Gassmann) behavior of porous rocks at low frequencies (sonic and below).

First new method of data display

In order to separate effects of liquids on λ from the well-understood effects of liquids on ρ, while taking advantage of the fluid-effect independence of μ, we will combine the v_p and v_s data into a new type of plot. For porous materials that satisfy Gassmann's conditions and low enough frequencies, we expect that, if we were instead to plot seismic velocity data in a two-dimensional array with one axis being $\rho/\mu = 1/v_s^2$ and the other being the ratio $\lambda/\mu = (v_p/v_s)^2 - 2$, then the result should be a straight (horizontal) line until $S \simeq 1$ (around 95% or higher), where the data should quickly rise

to a value determined by the velocities at full liquid saturation. This behavior is observed in Fig. 1b. Note that, although this behavior is qualitatively similar to that of v_p in Fig. 1a, we are now using only the seismic velocities themselves (no saturation data are required to generate this plot). What we observe here are traditional Gassmann-Domenico (Gassmann, 1951; Domenico, 1976) predictions for partial saturation.

If all the other assumptions of the Gassmann model are satisfied, but the liquid and gas are not distributed uniformly, then we have the circumstances that may better fit a fully segregated model. In that case, on a plot of λ/μ vs. ρ/μ, the data should lie on another straight line connecting the two end points (dry and fully saturated). These straight lines have been superimposed on the plots for Figs. 1c and 1d. The anticipated behavior is observed in Fig. 1c but not in 1d.

The apparent discrepancies from expected behavior are resolved by including another display for these two sandstones in Figs. 1e,f. Now the ratio λ/μ is plotted versus *saturation* measured in the laboratory, and we observe in all these cases that the basic plot structure we had anticipated for Figs. 1c and 1d is in fact confirmed. What we learn from this observation is that the quantity ρ/μ, that we wanted to use as a proxy for the saturation S, is not a very good proxy at ultrasonic frequencies. We can safely attribute the discrepancies in Fig. 1d to effects of high frequency dispersion as predicted by Biot's theory. Even the seemingly odd negative slope of the patchy saturation lines in Fig. 1d can be understood as a predicted high frequency effect on the shear velocity (Berryman, 1981).

This first new plotting method is limited by the implicit assumptions that the shear modulus is independent of the presence of fluids and that frequency dispersion for shear velocity is negligible. The assumption that the materials' shear properties are independent of the fluid is based on theoretical predictions about mechanical behavior only, and any chemical interactions between fluid and rock that might soften grain contacts could easily account for some of these discrepancies. Fluid-induced swelling of interstitial and intergranular clays is another possible source of discrepancy as is fluid-induced pressure effects if the fluid is overpressured and therefore tending to weaken the rock severely. All of the chemical effects mentioned should become active with even very small amounts of fluid present, and should not have any significant frequency dependence. On the other hand, there are frequency dependent (dispersion) effects predicted by Biot's theory of acoustics in porous media that can lead to complications difficult to resolve with the severely frequency-band limited data that are normally available.

Another new method of data display.

Now consider plotting the data points alternatively in the $(\rho/\lambda,\ \mu/\lambda)$-plane. In what was the straight-line portion of the curve in Fig. 1b, the only effect in the new plot will be a change of scale, but large changes will result in the points representing full saturation or nearly full saturation. The results of this new plotting method are displayed in Fig. 2. We observe that in all cases the result is apparently a straight line. This linear behavior is expected for a Gassmann material, since λ is just a scaling factor, μ is unaffected by saturation, and ρ is linearly dependent on saturation. It would also be expected for a non-Gassmann material in which the effect of fluids on λ was negligible compared to the effect on μ. It may also be expected for the case of patchy saturation if chemical interactions cause μ to change with saturation, because then μ for the porous medium would be some weighted average of μ for the dry case and μ for the fully saturated and chemically altered portions of the rock.

This straight line correlation is a very robust feature of partial saturation data. Numerous other examples of the correlation have been observed. No examples of appropriate data for partially saturated samples with major deviations from this behavior have been observed, although an extensive survey of available data sets has been performed for materials including limestones, sandstones, granites, unconsolidated sands, and some artificial materials such as ceramics and glass beads. The mathematical trick that brings about this behavior will be discussed below.

Porosity correlation

An additional feature of displays of the type presented in Fig. 2 is that the slopes of the straight lines, at least for samples of similar material character, are inversely correlated with the porosity of the samples. This observation is highlighted in Fig. 2b, where a series of fused glass-bead samples of uniform composition were produced (Berge *et al.*, 1995). The porosities are distributed almost perfectly in Fig. 2b, with the lower porosity lines having higher slopes and higher porosity lines having lower slopes to within the uncertainty of the laboratory measurments of porosity ($\pm 0.6\%$).

Linearity

We can understand both the linearity and the apparent dependence of the data correlation on porosity in the second plotting method by understanding some simple facts about such displays. Consider a random variable X. If we display data on a plot of either X vs. X or $1/X$ vs. $1/X$, the result will always be a perfect straight line. In both cases the slope of the straight line is exactly unity and the intercept of the line is the origin of the plot (0, 0). Now, if we have another variable Y and plot Y/X vs. $1/X$, then we need to consider two pertinent cases: (1) If $Y = constant$, then the plot of Y/X vs. X will again be a straight line and the intercept will again be the origin, but the slope will be Y, rather than unity. (2) If $Y \neq constant$ but is a variable with small overall variation (small dynamic range), then the plot of Y/X vs. $1/X$ will not generally be exactly a straight line. The slope will be given approximately by the average value

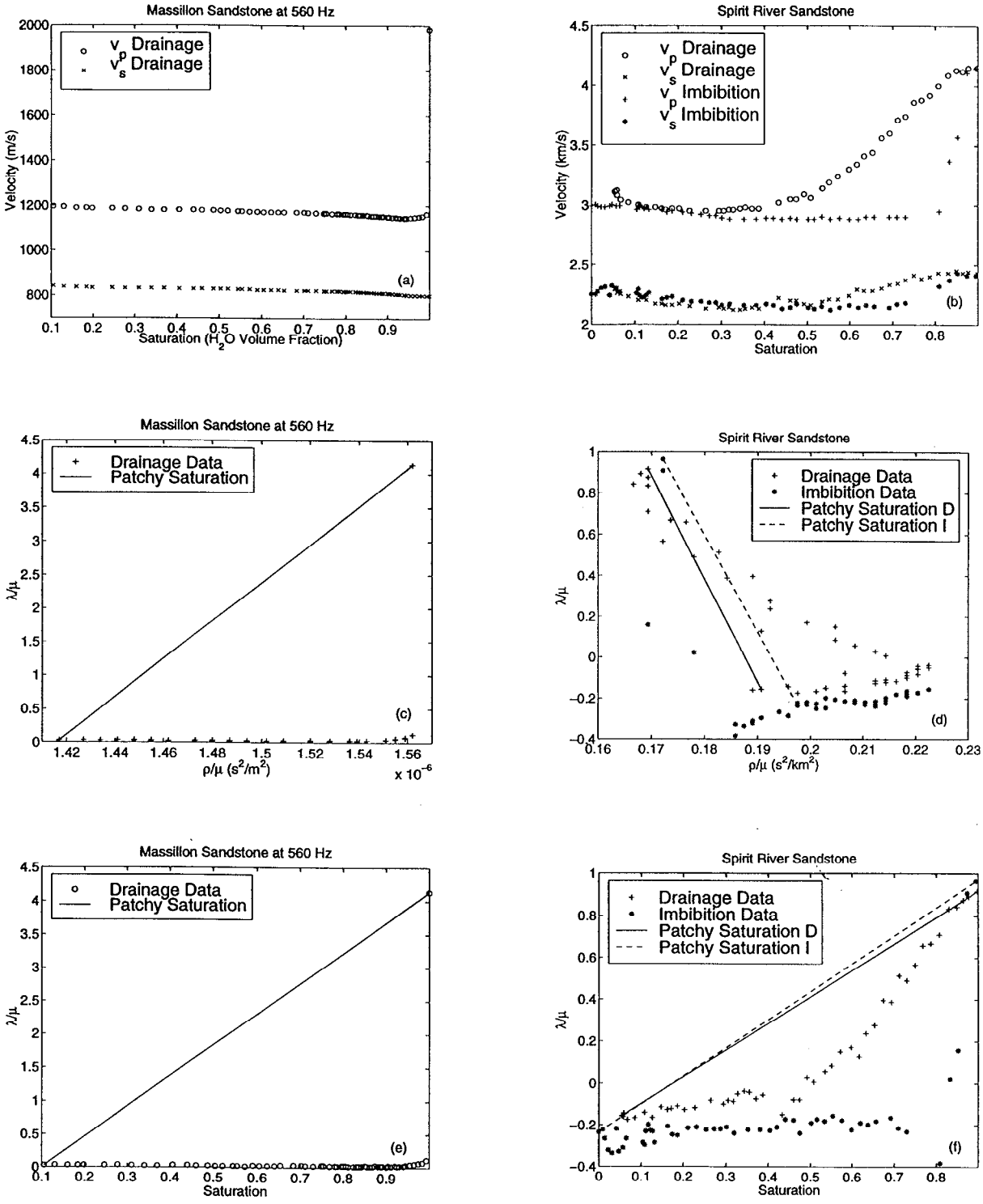

Figure 1: Compressional and shear velocities for Massilon sandstone measured by Murphy (1984) and for Spirit River sandstone measured by Knight and Nolen-Hoeksema (1990).

of Y and the intercept will be near the origin, but its precise value will depend on the correlation (if any) of Y and X. In our second method of plotting, the variable λ/ρ plays the role of X and the variable $v_s^2 = \mu/\rho$ plays the role of Y. The plots are approximately linear because this method of display puts the most highly variable combination of constants λ/ρ in the role of X, and the least variable combination of constants v_s^2 in the role of Y. Furthermore, the slope of the observed lines is therefore correlated inversely with the porosity ϕ because the slope is approximately the average value of v_s^2.

Conclusions

The new plotting methods described in this paper are promising methods for estimating both porosity and saturation from seismic data for complicated earth materials, whether or not they fit Gassmann's model or the patchy saturation model. High frequency data considered here are more likely to present wave attenuation and dispersion effects that normally complicate these analyses, but apparently do not seriously affect our interpretations when they are based on Lamé's constant λ as long as the data are taken in a range of frequencies that avoids the large dispersive effects. Porosity is correlated inversely with the slopes of the lines in Fig. 2.

Acknowledgments

We thank Bill Murphy and Rosemarie Knight for providing access to their unpublished data. We thank Norman H. Sleep for his insight clarifying the significance of our second method of plotting seismic data. Work performed under the auspices of the U. S. DOE LLNL under contract No. W-7405-ENG-48.

References

Berge, P. A., Bonner, B. P., and Berryman, J. G., 1995, Ultrasonic velocity-porosity relationships for sandstone analogs made from fused glass beads: *Geophysics*, **60**, 108–119.

Berryman, J. G., 1981, Elastic wave propagation in fluid-saturated porous media: *J. Acoust. Soc. Am.*, **69**, 416–424.

Biot, M. A., Mechanics of deformation and acoustic propagation in porous media. *J. Appl. Phys.* **33**, 1482–1498 (1962).

Domenico, S. N., 1976, Effect of brine-gas mixture on velocity in an unconsolidated sand reservoir: *Geophysics*, **41**, 882–894.

Gassmann, F., 1951, Über die elastizität poröser medien: *Vierteljahrsschrift der Naturforschenden Gesellschaft in Zürich*, **96**, 1–23.

Knight, R., & Nolen-Hoeksema, R., 1990, A laboratory study of the dependence of elastic wave velocities on pore scale fluid distribution: *Geophys. Res. Lett.*, **17**, 1529–1532.

Murphy, William F., III, 1984, Acoustic measures of partial gas saturation in tight sandstones: *J. Geophys. Res.*, **89**, 11549–11559.

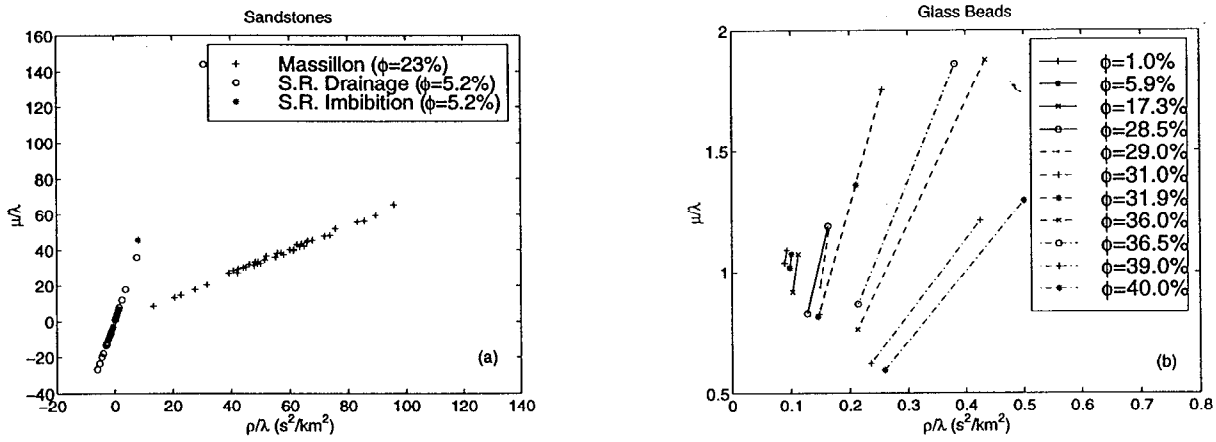

Figure 2: Examples of the correlation of slopes with porosity: (a) two sandstones (Murphy, 1984; Knight and Nolen-Hoeksema, 1990) and (b) 11 fused glass-bead samples (Berge *et al.*, 1995). The observed trend is that high porosity samples generally have lower slopes.